

AD-A042 057

NAVAL RESEARCH LAB WASHINGTON D C

F/G 4/1

COMMENTS ON CERTAIN BOUNDARY LAYER PARAMETERIZATION SCHEMES USE--ETC(U)

JUL 77 T YU, R MADALA

NRL-MR-3548

NL

UNCLASSIFIED

| OF |
ADAO42057



END

DATE
FILMED
8 - 77

ADA 042057

12
NW

NRL Memorandum Report 3548

Comments on Certain Boundary Layer Parameterization Schemes Used in Atmospheric Circulation Models

TSANN-WANG YU

JAYCOR
205 S. Whiting Street
Alexandria, VA 22304

RAO MADALA

Plasma Dynamics Branch
Plasma Physics Division

DDC
JUL 27 1977

July 1977

A

AD No. _____
DDC FILE COPY



ACCESSION for	
NTIS	White Section <input checked="" type="checkbox"/>
DDC	Buff Section <input type="checkbox"/>
UNANNOUNCED	<input type="checkbox"/>
JUSTIFICATION	
BY _____	
DISTRIBUTION AVAILABILITY CODES	
Dist.	SPECIAL

NAVAL RESEARCH LABORATORY
Washington, D.C.

SECURITY CLASSIFICATION OF THIS PAGE (When Data Entered)

REPORT DOCUMENTATION PAGE		READ INSTRUCTIONS BEFORE COMPLETING FORM
1. REPORT NUMBER NRL Memorandum Report 3548 ✓	2. GOVT ACCESSION NO.	3. RECIPIENT'S CATALOG NUMBER ⑨
4. TITLE (and Subtitle) COMMENTS ON CERTAIN BOUNDARY LAYER PARAMETERIZATION SCHEMES USED IN ATMOSPHERIC CIRCULATION MODELS		5. TYPE OF REPORT & PERIOD COVERED Interim report on a continuing NRL problem.
7. AUTHOR(s) ⑩ Tsann-Wang Yu, JAYCOR and Rao/Madala, NRL		6. PERFORMING ORG. REPORT NUMBER
9. PERFORMING ORGANIZATION NAME AND ADDRESS Naval Research Laboratory ✓ Washington, D.C. 20375		8. CONTRACT OR GRANT NUMBER(s) ⑭ NRL-MR-3548
11. CONTROLLING OFFICE NAME AND ADDRESS ⑫ 29p. ⑪		10. PROGRAM ELEMENT PROJECT, TASK AREA & WORK UNIT NUMBERS NRL Problem A03-23
14. MONITORING AGENCY NAME & ADDRESS (if different from Controlling Office)		12. REPORT DATE July 1977
		13. NUMBER OF PAGES 28
		15. SECURITY CLASS. (of this report) UNCLASSIFIED
		15a. DECLASSIFICATION/DOWNGRADING SCHEDULE
16. DISTRIBUTION STATEMENT (of this Report) Approved for public release; distribution unlimited.		
17. DISTRIBUTION STATEMENT (of the abstract entered in Block 20, if different from Report)		
18. SUPPLEMENTARY NOTES		
19. KEY WORDS (Continue on reverse side if necessary and identify by block number) Atmospheric boundary layer Numerical modeling Dynamic meteorology		
20. ABSTRACT (Continue on reverse side if necessary and identify by block number) This paper discusses two important processes of boundary layer parameterization for use in general circulation models (GCM). The first process, based on the surface constant flux layer theory, is applicable when the first level of a GCM is placed below the surface layer. The second one, based on the Rossby number similarity and generalized similarity theories, is appropriate when the first level of a GCM is above the entire boundary layer. Observation data taken from the Wangara and Kansas field experiments were used to analyze the (Continues)		

DD FORM 1 JAN 73 1473

EDITION OF 1 NOV 65 IS OBSOLETE
S/N 0102-014-6601

SECURITY CLASSIFICATION OF THIS PAGE (When Data Entered)

251 950

next page
mt

20. Abstract (Continued)

cont. effect of varying constant flux layer height (CFL) on the surface fluxes computation. Results of analyses with several cases of CFL effects are discussed. Parameterization of the atmosphere boundary layer by the Rossby number and generalized similarity theories is described, and the computations of boundary layer fluxes by these theories are compared.



CONTENTS

1. INTRODUCTION 1

2. PARAMETERIZATION BASED ON THE SURFACE
LAYER SIMILARITY THEORY 2

A. Constant Flux Layer Theory 2

B. Analysis Procedure 4

C. Analysis Results 5

3. PARAMETERIZATION BASED ON THE MATCHING OF
SURFACE AND OUTER LAYER SIMILARITY THEORIES ... 7

A. Determination of the Similarity Functions 8

B. Surface Fluxes Calculated by the Generalized Similarity
and Rossby Number Similarity Theories 11

4. SUMMARY AND CONCLUSIONS 13

ACKNOWLEDGEMENTS 15

REFERENCES 16

ACCESSION	
NTIS	Write Section <input checked="" type="checkbox"/>
DDC	Buff. Section <input type="checkbox"/>
UNANNOUNCED	<input type="checkbox"/>
JUSTIFICATION	
BY	
DISTRIBUTION AVAILABILITY CODES	
Dist.	AVAIL and/or SPLICED
A	

COMMENTS ON CERTAIN BOUNDARY LAYER PARAMETERIZATION SCHEMES USED IN ATMOSPHERIC CIRCULATION MODELS

1. INTRODUCTION

The structure of the atmospheric boundary layer is characterized by two distinct sublayers. Immediately above the surface up to approximately 30 m height the vertical variation of eddy stress and other fluxes can be neglected, and the wind direction is essentially constant. This layer is called the surface layer, or alternatively the constant flux layer. The height of the constant flux layer is quite variable. At night, when fluxes are weak and the stratification strong, the stress may be constant for only a few meters near the surface. At the other extreme, during the daytime convective periods, there is strong turbulent mixing. Thus the surface layer may extend to a considerable height above the surface. Above the constant flux layer is the Ekman layer, or the outer layer. In this layer, the earth's rotation and the large scale pressure gradients in addition to the eddy stresses are important in controlling the wind and temperature profiles. The turbulent fluxes typically decrease upward within the outer layer.

The interaction between the boundary layer and the free atmosphere occurs through the vertical fluxes of momentum, mass, heat and moisture, and the frictional dissipation within the boundary layer. The essential purpose of boundary layer parameterization is to generate simple models for the computation of the boundary layer fluxes. The first part of this paper discusses the parameterizations based on the surface layer similarity theory. This theory is applicable whenever the first

grid level of a general circulation model can be placed within the constant flux (or surface) layer. In particular, we shall examine the effect of varying the constant flux layer height on the computation of the boundary layer fluxes. The second part of this paper concerns parameterization of the whole planetary boundary layer. This is necessitated by the fact that many large scale models have such poor vertical resolution that the first interior grid point level is well above the top of the surface layer. The boundary layer fluxes in this case are calculated by the so-called Rossby number similarity theory or generalized similarity theory with empirically determined similarity functions. According to the similarity theories, these empirical functions depend on the surface Monin-Obukhov length which is impractical to determine. However, a bulk Richardson number which is closely related to the Monin-Obukhov length can be explicitly determined. Thus, we shall specifically discuss how the similarity functions can be determined by the bulk Richardson number approach. Moreover, we shall compare the computed boundary layer fluxes of the generalized similarity theory and the Rossby similarity theory.

2. PARAMETERIZATION BASED ON THE SURFACE LAYER SIMILARITY THEORY

A. Constant Flux Layer Theory

In this section, we shall discuss computation of surface fluxes of heat and momentum based on flux-profile relationships as established through the Monin-Obukhov similarity theory. The most complete characterization of fluxes and profiles comes from the Kansas experiments, as published by Businger et al. (1971).

Following Businger et al. (1971), we define the following dimensionless quantities:

$$R_i = \frac{g\bar{\theta}/\partial Z}{\bar{\theta}(\partial\bar{u}/\partial Z)^2}$$

Richardson number, a stability parameter

$$\phi_m = \frac{kZ}{u_*} \frac{\partial\bar{u}}{\partial Z}$$

A dimensionless wind shear

$$\phi_\theta = \frac{kZ}{\theta_*} \frac{\partial\bar{\theta}}{\partial Z}$$

A dimensionless temperature gradient

$$\xi = \frac{Z}{L} = - \frac{kg\bar{w}'\bar{\theta}'Z}{\bar{\theta}u_*^3}$$

A dimensionless height

where

- g = acceleration due to gravity
- k = von Kármán's constant = (0.35)
- u, v, w = longitudinal, lateral and vertical components of the wind
- \bar{u} = magnitude of the mean horizontal wind vector
- Z = vertical coordinate
- θ = potential temperature
- u_* = friction velocity $\{(\tau_0/\rho)^{1/2}\}$
- θ_* = scaling temperature $\{-\overline{w'\theta'}/(ku_*)\}$
- L = Obukhov length $\{-\bar{\theta}u_*^3/(kg\overline{w'\theta'})\}$
- ρ = air density
- τ_0 = surface shearing stress
- C_p = specific heat of air at constant pressure

Based on the experimental results of Businger et al. (1971), the

universal functions ϕ_m and ϕ_θ can be written as:

$$\phi_m = \begin{cases} (1 - 15\xi)^{-\frac{1}{4}}, & \xi < 0 \text{ (unstable)} \\ 1 + 4.7\xi, & \xi \geq 0 \text{ (stable)} \end{cases}$$

$$\phi_\theta = \begin{cases} 0.74(1 - 9\xi)^{-\frac{1}{2}}, & \xi < 0 \text{ (unstable)} \\ 0.74 + 4.7\xi, & \xi \geq 0 \text{ (stable)} \end{cases}$$

The procedure involves the computation of the surface shearing stress τ_0 and heat flux, $\rho C_p u_* \theta_*$, for a given set of wind and temperature profiles between Z and surface roughness height Z_0 . The height of the surface or constant flux layer Z is quite variable as it was pointed out previously. As a result, an assumed height of the surface layer can have great effects on the computation of the surface shearing stress and heat fluxes. Here we attempt to assess the effects on the surface fluxes of momentum and heat based on experimental data when different constant flux layer heights are assumed.

B. Analysis Procedure

Data used for the analyses are based on the Wangara (Clarke et al., 1971), and the Kansas (Izumi, 1968) field experiments. From the Wangara data, 40 days of wind and temperature measurements at four levels, i.e. 50 m, 4 m, 2 m, and 1.2 m were chosen. From the Kansas data, hourly values of wind and temperature at five levels, i.e. 32 m, 16 m, 8 m, 4 m, and 1 m were selected.

Only a brief account of the computation procedure of the surface fluxes will be given here. For details the reader is referred to

Barker and Baxter (1975). First, the bulk Richardson number was calculated from the wind and temperature profile data. Next, the surface Obukhov length was deduced on the assumption that an individual vertical flux and its associated vertical gradient strictly obey the empirical relationships of Businger et al. (1971). Then, the surface friction velocity, and thus surface shearing stress, were calculated from the integrated form of the empirical diabatic wind shear relationship, using observed wind speeds at selected heights. It should be noted that no assumption was made on the value of the surface roughness length. Lastly, the heat flux, and thus the kinematic heat flux, are obtained from the flux gradient relationship of Businger et al. (1971) using the calculated values of friction velocity.

C. Analysis Results

Fig. 1 shows the results of the analyses based on the Wangara data. Eight day's results are presented. These are typical of the 40 day's results of the Wangara data. The most striking features occur during the convective hours, i.e., 1200 and 1500. The shearing stress (top) and heat fluxes (bottom) calculated using wind and temperature profiles at $Z_1 = 1.2$ m and $Z_2 = 50$ m show great discrepancies when compared to those calculated with profiles taken from $Z_1 = 1.2$ m and $Z_2 = 2$ m. We speculate that if wind and temperature profiles at a height of 50 m (or greater) were used, the very super-adiabatic layer existing near the ground during the convective hours may not be reflected in the calculation of a bulk Richardson number. As a consequence, the Obukhov lengths are calculated to be of nearly neutral values, and thus the fluxes calculated are much too small in magnitude. However,

if wind and temperature at a height lower than 2 m are used, then measurement errors in the data will probably lead to inaccurate flux calculations. Note that both shear stress and heat fluxes calculated with $Z_1 = 1.2$ m and $Z_2 = 4$ m compare well with those of Melgarejo and Deardorff (1975).

The 1968 Kansas surface layer data include independent measurements of both surface friction velocity and heat fluxes. Thus, the calculated results can be easily compared with the measured values. Four cases are considered. Case A: the height of the constant flux layer (CFL) is set to be 4 m with wind and temperature profiles taken at two levels i.e., $Z_1 = 1$ m, and $Z_2 = 4$ m. Case B: CFL = 8 m, $Z_1 = 1$ m and $Z_2 = 8$ m. Case C: CFL = 16 m, $Z_1 = 1$ m, $Z_2 = 16$ m. Case D: CFL = 32 m, $Z_1 = 1$ m and $Z_2 = 32$ m. The calculation of surface friction velocity and kinematic heat flux are done in the same way as for the Wangara data described previously.

The calculated values for these four cases for the Kansas experiment are tabulated in Appendix I. The RMSE values (Root Mean Squares Errors) of the calculated surface friction velocity and kinematic heat flux with respect to the measured values are given in Table I. It can be seen from a comparison of the RMSE values given in Table I that the poorest results were obtained when wind and temperature profiles were taken with $Z_1 = 1$ m and $Z_2 = 4$ m (Case A). On the other hand, the best results in the calculation of surface friction velocity and kinematic heat flux come from Case D where wind and temperature data at $Z_1 = 1$ m and $Z_2 = 32$ m were taken. These results again suggest that if the height of a constant flux layer is assumed to be very shallow such as less than 4 m

depth, then any small measurement errors in wind and temperature profiles will lead to great inaccuracies in the calculation of surface shearing stress and heat fluxes.

The results of the above analyses are based on an assumption that the data taken from the Wangara and Kansas field experiments strictly followed the flux-profile relationships of Businger et al. (1971). A more stringent assumption was that all the data taken at any two levels would behave according to the surface similarity theory. These two assumptions might be responsible for the fact that great variability was exhibited in the surface flux calculations with different constant flux layer heights assumed in the analyses. For the purpose of parameterizing the atmospheric boundary layer for use in general circulation models, a fixed height of 10-30 m for the constant flux layer may be practical and reliable. However, for modeling detailed structures of the atmospheric boundary layer, a sensitivity analysis of the effect of different CFL heights is a necessity.

3. PARAMETERIZATION BASED ON THE MATCHING OF SURFACE AND OUTER LAYER SIMILARITY THEORIES

As pointed out previously, when a GCM has such a poor vertical resolution that the first interior grid level is well above the top of the surface layer, one must parameterize the whole boundary layer. The best forms of parametric relationship for this have been derived by the matching of mean profiles predicted by surface and outer layer similarity theories (Blackadar and Tennekes, 1968; Zilitinkevich, 1975). The general form of the drag (or surface shear stress) and heat transfer (or heat fluxes) relations obtained from similarity matching arguments

is,

$$ku_h/u_* = - (\ln \hat{Z}_0 + A)$$

$$kv_h/u_* = - B \text{ sign} \cdot f$$

$$k(\theta_h - \theta_0)/\theta_* = - (\ln \hat{Z}_0 + C)$$

$$k(q_h - q_0)/q_* = - (\ln \hat{Z}_0 + D)$$

where u and v are the horizontal components (in the direction of surface shear and perpendicular to it, respectively) of mean velocity vector (the subscript h refers to the variables at the top of the boundary layer), \hat{Z}_0 is the roughness parameter normalized by the scale height (h or u_*/f) of the boundary layer, and A , B , and C and D are some similarity functions.

A. Determination of the Similarity Functions

The purpose of this section is to describe how the similarity functions A , B and C can be determined by the bulk Richardson number. In theory, the similarity functions A , B and C are functions of atmospheric stability μ , where h is height of the planetary boundary layer and L is the surface Monin-Obukhov length defined as, $L = \bar{\theta} u_*^2 / kg \theta_*$. It is apparent that L is related to the internal parameters u_* and θ_* which are to be determined. Thus, it is not practical to determine similarity functions A , B and C in terms of L . Deardorff (1972) discussed the relationship between the geostrophic drag or heat transfer coefficients and the bulk stability (bulk Richardson number). Recently, Yamada (1976) reexamined the similarity functions based on the Wangara

data. Both in the stable and unstable conditions, his proposed universal functions $A(\mu)$, $B(\mu)$ and $C(\mu)$ show substantial improvement when compared with the observed data over the previous work by Deardorff and Melgarejo (1975) and Arya (1974). We shall thus reformulate the similarity functions in terms of bulk Richardson number based on Yamada's (1976) work.

The bulk Richardson number R_{iB} is related to similarity functions by

$$R_{iB} = 0.74 \frac{h}{L} \frac{\ln(h/Z_0) - C}{\{\ln(h/Z_0) - A^2\} + B^2}$$

where functions A , B and C are defined as in Yamada (1976). It follows that for a given set of values of $\zeta = h/L$ and roughness parameter Z_0 , the corresponding values of A , B , and C , and R_{iB} are readily determined. Now, for a given values of R_{iB} and Z_0 , we like to determine h/L and hence A , B , and C . For this purpose, the Newton-Ralphson method is useful,

$$\zeta_{i+1} = \zeta_i + \{R_{iB} - f(\zeta_i)\}/f'(\zeta_i),$$

where

$$f(\zeta) = 0.74\zeta(\alpha - c)/\{(\alpha - A)^2 + B^2\}$$

and

$$f'(\zeta) = f(\zeta_i)\{1/\zeta - c'/(\alpha - c) - 2(AA' - \alpha A' + BB')/\left[(\alpha - A)^2 + B^2\right]\}$$

where $\zeta \equiv h/L$ and $\ln(h/Z_0) \equiv \alpha$. The subscript i denotes the iteration index, and $()'$ the derivatives with respect to ζ .

The Newton-Ralphson method was tested both for stable and unstable cases of similarity functions A, B, and C based on Yamada (1976). We found for stable cases, i.e. $h/L > 0$, the Newton-Ralphson method converges within five iterations. Following Yamada (1976), the similarity functions for stable cases are:

$$(i) \quad 18 \leq \zeta \leq 0$$

$$A = 1.855 - .380\zeta, \quad A' = - .380$$

$$B = 3.020 + .300\zeta, \quad B' = .300$$

$$C = 3.665 - .819\zeta, \quad C' = - .819$$

$$(ii) \quad 35 \leq \zeta < 18$$

$$A = 1.855 - .380\zeta, \quad A' = - .380$$

$$B = 3.020 + .300\zeta, \quad B' = .300$$

$$C = - 4.32(\zeta - 11.21)^{\frac{1}{2}}, \quad C' = - 4.32(\zeta - 11.21)^{-\frac{1}{2}}$$

$$(iii) \quad \zeta > 35$$

$$A = - 2.94(\zeta - 19.94)^{\frac{1}{2}}, \quad A' = 1.47(\zeta - 19.94)^{-\frac{1}{2}}$$

$$B = 2.85(\zeta - 12.47)^{\frac{1}{2}}, \quad B' = 1.425(\zeta - 12.47)^{-\frac{1}{2}}$$

$$C = - 4.32(\zeta - 11.21)^{\frac{1}{2}}, \quad C' = 2.16(\zeta - 11.21)^{-\frac{1}{2}}$$

For unstable cases, a simple linear relationship occurs between the bulk Richardson number and ζ , i.e.,

$$\zeta = R_{iB} f(C_N)$$

where $C_N \equiv \frac{1}{k} \ln(h/Z_0)$, where k is von Kármán constant, and $f(C_N) = .75$

$C_N - 1$. Table 2 shows the values of A, B, and C based on these two

different methods. The values denoted with () are those calculated with given bulk Richardson numbers, and those without () are calculated based on given h/L . The agreement between these two methods are remarkable.

The geostrophic drag C_D and heat transfer coefficients C_H are defined as, (see Yamada, 1976)

$$C_D = k \{ (\ln(h/Z_0) - A)^2 + B^2 \}^{-\frac{1}{2}},$$

$$C_H = 1.35 k \{ \ln(h/Z_0) - C \}^{-1}$$

The calculated values of C_D and C_H based on the two different methods are shown in Fig. 2. Very close agreement in the values of C_D and C_H between the two methods are indicated.

B. Surface Fluxes Calculated by the Generalized Similarity and Rossby Number Similarity Theories

The difference between the generalized similarity and the Rossby number similarity theory is that the former assumes that the boundary layer height is uniquely determined by u_*^2/f and L (Obukhov length). In the generalized version h is considered as an independent variable (Zilitinkevich and Deardorff, 1974), therefore, in the latter the effects of complicated factors such as nonstationarity, diurnal heating, large-scale advection of heat and moisture, large-scale subsidence, etc. on which h depends in the real atmosphere, can be considered indirectly by specifying h through a rate equation (Deardorff, 1974).

In this section, we shall examine the surface fluxes calculation

based on these two theories. For this purpose, we shall use the observed data set taken from the Wangara experiment. In particular, those days of the Wangara experiment chosen by Melgarejo and Deardorff (1975) will be selected for analyses. The observed boundary layer height h_{θ} , defined as the height to which significant cooling had extended as judged both from individual profiles and their evolution in time, will be used to compute the surface fluxes of heat and momentum by generalized similarity theory. For the Rossby number similarity theory, two fixed values of h will be examined, i.e. $h = 1000$ m and $h = 500$ m. Determination of the various similarity functions are done by the empirical formulations of Yamada (1976). Specifically, the similarity functions are determined by the bulk Richardson number approach as described in Section 3A.

The calculated surface friction velocity and kinematic heat flux are listed in Appendix II. The Root Mean Square Errors (RMSE) of the calculated surface friction velocity u_* and kinematic heat flux $H_0/\rho C_p$ with respect to the values calculated in Melgarejo and Deardorff (1975) are shown in Table 3. It should be noted that the surface friction velocity and kinematic heat flux calculated in Melgarejo and Deardorff (1975) are based on the flux-profile relationship of Businger et al. (1971). As noted in Melgarejo and Deardorff (1975), the fluxes thus calculated were obtained from the observed wind and temperature gradients between 1 and 4 m. The fact that the surface similarity theory is well established and the profile-flux relationships of Businger et al. (1971) are well deduced from a carefully gathered field experiment justifies the use of the results of Melgarejo and Deardorff (1975) as the

comparison standard. From Table 3 and 4, we see that during the unstable period, the RMSE values for the generalized similarity theory are not much different from those for the Rossby similarity theories. This suggests that during the unstable period, the Rossby number similarity approach is equally valid as the generalized similarity theory. During the unstable period, wind and temperature profiles are typically well mixed throughout the top of the boundary layer (near 1500 m). As a consequence, little difference in the prediction by the three similarity theories may be expected. During the stable period, it is evident from Table 3 that the Rossby number similarity theory (especially with $h = 1000$ m) performs better than the generalized similarity theory. This effect may be due to the fact that the boundary layer heights are somewhat indeterminate at the stable hours so that the computation of boundary layer fluxes based on the generalized similarity theory may be subject to large errors. Based on this analysis, we must conclude that the Rossby similarity theory is useful and practical. Although the generalized similarity theory has more of a physical basis and is highly advocated by many researchers (see e.g. Deardorff, 1974, Arya, 1977, and many others), the advantages of the theory are not well reflected in these surface fluxes calculation. On the other hand, the Rossby similarity has certain practical advantages in the atmospheric circulation models. The main advantage is to use a fixed scale height as the top of the boundary layer from which the boundary layer fluxes may be computed.

4. SUMMARY AND CONCLUSIONS

This paper concludes that the height of the constant flux layer should

not be assumed to be greater than 50 m in a numerical model. This is because during the convective periods, the very super-adiabatic lapse rate normally existing near the ground may not be reflected in the calculation of a bulk Richardson number. As a result, the fluxes tend to be underestimated. On the other hand, if the height of a constant flux layer is assumed to be very shallow, i.e. less than four meters, then any small measurement errors in the wind and temperature profiles will lead to great inaccuracies in the calculation of surface shearing stress and heat fluxes. For numerical models of the atmospheric circulation, we recommend a constant flux layer of about 10-30 meters depths to be practical and reliable.

We describe how the similarity functions A, B, C, and D can be determined based on the bulk Richardson number and have demonstrated that the similarity functions based on a recent analyses of Yamada (1976) can be computed using a Newton-Ralphson iterative scheme during the stable period. During the unstable period, a linear relation is found between the bulk Richardson number and Obukhov length. The relationship is derived and the results of drag and heat transfer coefficients are found to be satisfactory. Analysis based on the Wangara data indicates that the Rossby number similarity theory is useful and practicable. Although the generalized similarity theory has a more physical basis, this analysis shows that parameterization of the boundary layer fluxes through the Rossby number theory is equally valid as is the generalized theory during the unstable period. During the stable period, the Rossby number similarity theory performs better than the generalized theory in the computation of the

boundary layer fluxes. However, it should be pointed out that the Rossby similarity theory may not be valid near the tropics where the determination of the boundary layer height by u_* / f is no longer valid. For this reason, the generalized similarity theory should be recommended for modeling the global circulations. For mid-latitude general circulation studies, the Rossby number similarity theory may be adequate.

ACKNOWLEDGEMENTS

The authors are grateful to Drs. Mark Schoeberl and Darrell Strobel of the Naval Research Laboratory for their reviews of the paper and to Margaret Mikota for typing the manuscript. This work has been supported by the Naval Air System Command Task No. WF 52-552-713.

REFERENCES

- Arya, S. P. S., 1975: Geostrophic drag and heat transfer relations for the atmospheric boundary layer. Quart. J. Roy. Meteor. Soc., 101, 147-161.
- Arya, S. P. S., 1977: Suggested revision to certain boundary layer parameterization schemes used in atmospheric circulation models. Mon. Wea. Review, 105, 215-227.
- Barker, E. H., and T. L. Baxter, 1975: A note on the computation of atmospheric surface layer fluxes for use in numerical modeling. J. Appl. Met. 14, 620-622.
- Blackadar, A. K., and H. Tennekes, 1968: Asymptotic similarity in neutral barotropic planetary boundary layers. J. Atmos. Sci., 25, 1015-1020.
- Businger, J. A., J. C. Wyngarrd, Y. Izumi, and E. F. Bradley, 1971: Flux-profile relationships in the atmospheric surface layer. J. Atmos. Sci., 28, 181-189.
- Clarke, R. H., A. J. Dyer, R. R. Brook, D. G. Reid, and A. J. Troup, 1971: The Wangara Experiment: Boundary Layer Data. Commonwealth Scientific and Industrial Research Organization, Australia, 1971, 349 pp.
- Deardorff, J. W., 1972: Parameterization of the planetary boundary layer for use in general circulation models. Mon. Wea. Rev. 100, 93-106.
- Izumi, U., 1971: Kansas 1968 Field Program Data Report. Environmental Research Paper No. 379, AFCRL-72-0041 (Available from NTIS as AD-739-165).
- Melgarejo, J. W., and J. W. Deardorff, 1974: Revision to "Stability Functions for the boundary-layer resistance laws based upon observed boundary-layer height." J. Atmos. Sci., 32, 837-839.
- Yamada, T., 1976: On the similarity functions A, B and C of the Planetary boundary layer. J. Atmos. Sci., 33, 781-793.
- Zilitinkevich, S. S., 1975: Resistance laws and prediction equations for the depth of the planetary boundary layer. J. Atmos. Sci., 32, 741-752.
- Zilitinkevich, S. S., and J. W. Deardorff, 1974: Similarity theory for the planetary boundary layer of time-dependent height. J. Atmos. Sci., 31, 1449-1452.

Table 1: RMSE (Root Mean Square Errors) of the Calculated Surface Friction Velocity (m s^{-1}) and Kinematic Heat Flux ($\text{m s}^{-1} \text{ } ^\circ\text{K}$) for the Kansas Experiment Data

	Case A (constant flux layer height, i.e., CFL = 4 m; and $Z_1 = 1 \text{ m}$, $Z_2 = 4 \text{ m}$)	Case B (CFL = 8 m, $Z_1 = 1 \text{ m}$, $Z_2 = 8 \text{ m}$)	Case C (CFL = 16 m, $Z_1 = 1 \text{ m}$, $Z_2 = 16 \text{ m}$)	Case D (CFL = 32 m, $Z_1 = 1 \text{ m}$, $Z_2 = 32 \text{ m}$)
Friction Velocity (m s^{-1})	0.054	0.024	0.020	0.018
Kinematic Heat Flux ($\text{m s}^{-1} \text{ } ^\circ\text{K}$)	0.033	0.024	0.022	0.020

Table 2: Similarity functions A, B and C
 $h/z_0 = 10^5$

h/L	A	B	C	R_{iB}	(h/L)	(A)	(B)	(C)
-2	1.90	1.54	3.83	-.12	-2.4	1.91	1.45	3.87
-10	2.07	0.93	4.38	-.59	-11.9	2.11	0.88	4.50
-18	2.23	0.77	4.82	-1.03	-21.0	2.28	0.73	4.95
-26	2.37	0.68	5.16	-1.46	-29.7	2.44	0.65	5.30
-38	2.57	0.60	5.57	-2.08	-42.4	2.64	0.58	5.70
-60	2.89	0.52	6.13	-3.20	-65.3	2.96	0.50	6.24
-100	3.35	0.44	6.79	-5.22	-106.5	3.41	0.43	6.88
-140	3.71	0.39	7.23	-7.27	-148.1	3.78	0.38	7.31
-180	4.00	0.36	7.55	-9.33	-190.2	4.07	0.35	7.62
-250	4.41	0.32	7.96	-13.01	-265.2	4.48	0.32	8.03
-340	4.80	0.29	8.31	-17.84	-363.6	4.89	0.28	8.39
-510	5.32	0.75	8.75	-27.16	-553.6	5.42	0.25	8.83

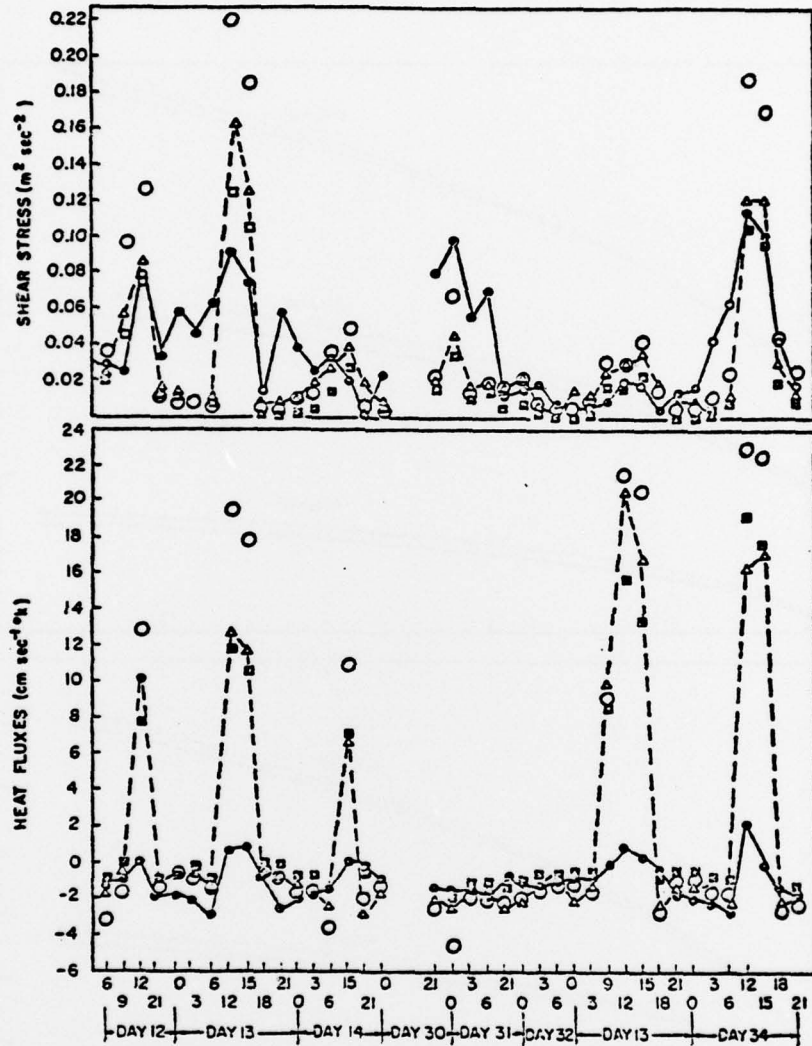
Values with () are calculated from bulk Richardson number.

Table 3: RMSE (Root Mean Square Errors) of the Calculated Surface Friction Velocity u_* (cm s^{-1}) and Kinematic Heat Flux $H_0/\rho C_p$ ($\text{cm s}^{-1} \text{ }^\circ\text{K}$) with Respect to the Values Calculated in Melgarejo and Deardorff (1975) for the Wangara Experiment Data.

	Generalized Similarity		Rossby with $h = 1000 \text{ m}$		Rossby with $h = 500 \text{ m}$	
	u_*	$H_0/\rho C_p$	u_*	$H_0/\rho C_p$	u_*	$H_0/\rho C_p$
Unstable Period	4.1	23.55	6.3	22.64	4.5	23.37
Stable Period	21.1	36.96	9.8	5.41	14.6	19.52

Table 4: Calculated Means and Standard Errors of Surface Friction Velocity u_* (cm s⁻¹) and Kinematic Heat Flux $Ho/\rho C_p$ (cm s⁻¹ °K) for the Wangara Experiment Data

	Generalized Similarity		Rossby with h=1000 m		Rossby with h=500		Melgarejo and Deardorff (1975)	
	u_*	$Ho/\rho C_p$	u_*	$Ho/\rho C_p$	u_*	$Ho/\rho C_p$	u_*	$Ho/\rho C_p$
Unstable Period N=17	24.1 (1.65)	27.95 (4.70)	23.3 (1.92)	23.89 (5.28)	23.5 (1.94)	28.11 (4.55)	25.2 (2.28)	9.9 (1.30)
Stable Period N=61	24.0 (2.42)	-24.98 (3.64)	5.8 (1.43)	-1.64 (.73)	13.6 (2.24)	-8.9 (2.32)	10.2 (.73)	-.89 (.08)



○ : indicates values calculated by assuming a Constant Flux Layer(CFL) of 2 m and using wind and temperatures at two levels $Z_1 = 1.2$ m and $Z_2 = 2$ m. Δ : CFL = 4 m, $Z_1 = 1.2$ m and $Z_2 = 4$ m. ● : CFL = 50 m, $Z_1 = 1.2$ m and $Z_2 = 50$ m. ■ Melgarejo and Deardorff (1975).

Fig. 1 — Surface shearing stress (top) and kinematic heat flux (bottom) calculated with three different wind and temperature profiles for eight selected days of the Wangara Experiment

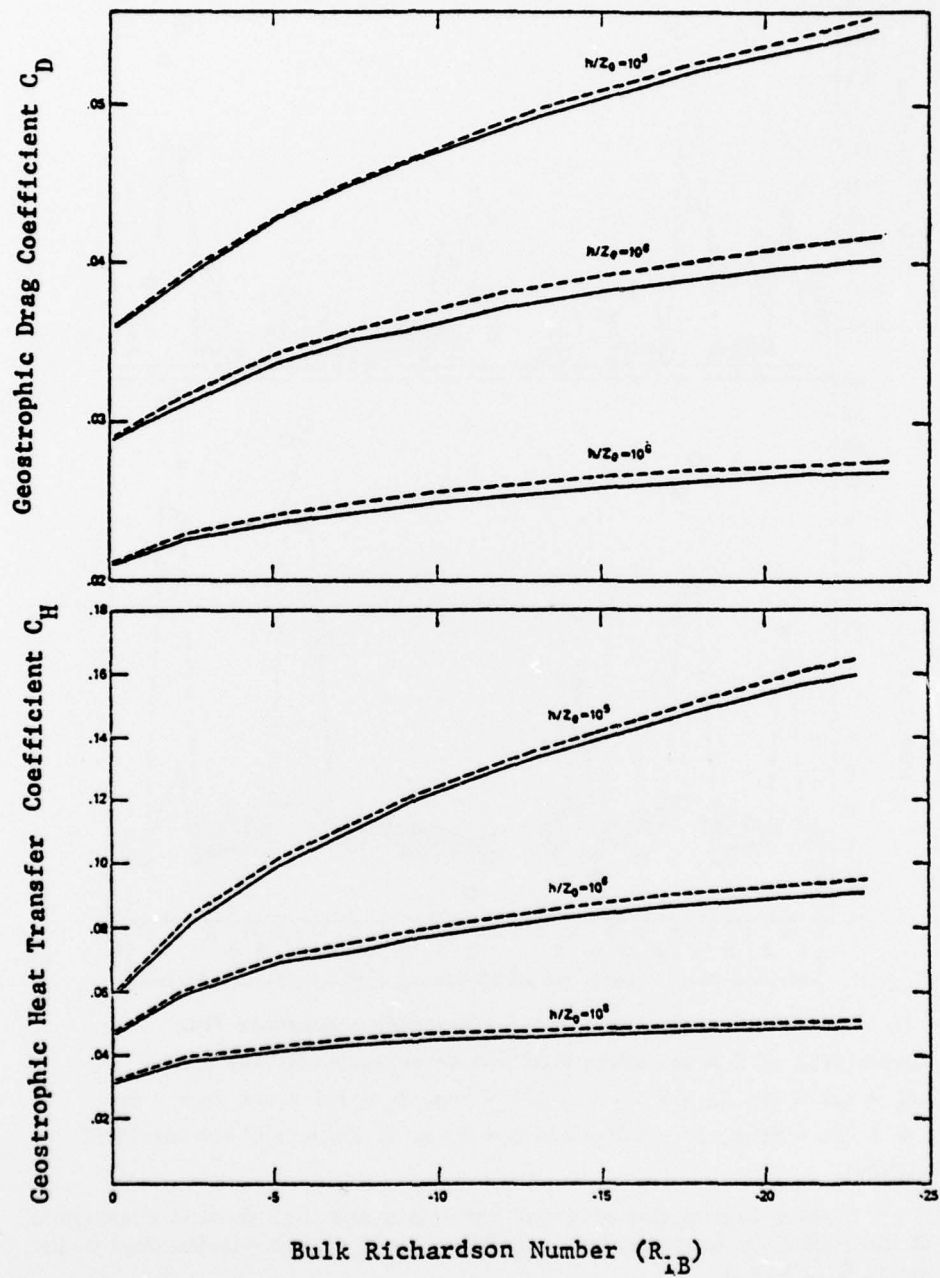


Fig. 2 — Geostrophic drag coefficient C_D (top) and geostrophic heat transfer coefficient C_H (bottom) calculated by given h/L values (solid lines) and by the Bulk Richardson number approach (dashed lines)

APPENDIX 1: Measured and Calculated Kinematic Heat Flux ($m s^{-1} \text{ } ^\circ K$)
and Surface Friction Velocity ($m s^{-1}$) for the Kansas Experiment Data

Run No.	Surface Friction Velocity ($m s^{-1}$)					Kinematic Heat Flux ($m s^{-1} \text{ } ^\circ K$)				
	Measured	Case A	Case B	Case C	Case D	Measured	Case A	Case B	Case C	Case D
8	0.40	.455	.433	.425	.424	.182	.241	.204	.196	.201
13	0.43	.475	.467	.459	.450	.212	.251	.213	.218	.215
14	0.39	.465	.436	.433	.427	.217	.469	.342	.314	.299
17	0.20	.203	.186	.189	.199	-.020	-.017	-.017	-.017	-.017
18	0.34	.341	.330	.332	.344	-.031	-.025	-.024	-.026	-.027
19	0.29	.332	.308	.315	.313	.202	.244	.203	.182	.192
20	0.36	.421	.400	.395	.393	.262	.293	.244	.242	.248
21	0.44	.473	.471	.473	.472	.146	.172	.155	.151	.155
22	0.17	.164	.163	.175	.174	-.017	-.019	-.017	-.019	-.017
23	0.08	.118	.086	.107	.149	-.006	-.015	-.008	-.012	-.022
24	0.18	.181	.168	.183	.180	-.019	-.019	-.016	-.018	-.017
25	0.24	.235	.230	.246	.259	-.023	-.020	-.020	-.024	-.026
26	0.21	.226	.216	.240	.252	-.019	-.018	-.017	-.022	-.026
28	0.32	.317	.315	.312	.319	.263	.300	.271	.260	.256
29	0.36	.362	.366	.369	.362	.166	.208	.188	.187	.180
30	0.33	.325	.334	.329	.332	.137	.141	.134	.130	.132
31	0.36	.366	.372	.363	.356	.052	.055	.048	.047	.046
32	0.42	.376	.395	.389	.365	-.015	-.021	-.020	-.018	-.015
33	0.36	.297	.318	.321	.324	-.024	-.021	-.020	-.020	-.019
34	0.36	.305	.314	.323	.325	-.020	-.020	-.020	-.020	-.020
37	0.29	.258	.251	.253	.268	-.029	-.023	-.022	-.023	-.024
38	0.26	.240	.225	.229	.229	-.025	-.021	-.018	-.019	-.018
40	0.41	.442	.423	.419	.404	.191	.234	.192	.193	.197
42	0.48	.488	.467	.479	.478	.288	.332	.284	.296	.289
43	0.48	.489	.468	.470	.478	.206	.281	.213	.223	.228
45	0.33	.342	.327	.324	.324	.221	.241	.205	.212	.209
46	0.31	.327	.312	.311	.306	.246	.264	.249	.238	.232
47	0.33	.351	.335	.329	.334	.173	.173	.162	.156	.153
48	0.41	.438	.424	.425	.414	.131	.170	.153	.157	.155
49	0.45	.498	.486	.466	.454	.013	.007	.012	.012	.015
53	0.46	.489	.473	.474	.485	.123	.190	.143	.147	.148
54	0.52	.528	.532	.509	.519	.070	.107	.067	.073	.071

APPENDIX II: Surface Friction Velocity u_* (cm s^{-1}) and Kinematic Heat Flux $Ho/\rho C_p$ ($\text{cm s}^{-1} \text{ } ^\circ\text{K}$) Calculated by the Generalized Similarity and Rossby Number Similarity Theories for the Wangara Experiment Data

Day	Hour	Generalized Similarity		Rossby, $h=1000$ m		Rossby, $h=500$ m		Melgarejo & Deardorff (1975)	
		u_*	$Ho/\rho C_p$	u_*	$Ho/\rho C_p$	u_*	$Ho/\rho C_p$	u_*	$Ho/\rho C_p$
STABLE PERIOD									
1	6	14.5	-7.49	1.0	-.06	1.6	-.16	5.5	-.35
	18	31.1	-26.65	6.5	-.80	14.1	-3.42	11.0	-1.24
	21	38.0	-42.57	11.8	-2.62	22.3	-9.29	12.4	-1.10
	24	47.5	-61.66	8.6	-1.75	44.2	-55.5	16.5	-1.42
4	3	46.7	-41.88	11.4	-2.42	45.5	-42.1	14.2	-1.24
	6	41.5	-39.48	10.0	-1.97	41.8	-39.7	15.8	-1.77
6	18	6.4	-1.39	0.2	-.00	0.8	-.03	5.8	-.52
	21	10.1	-4.12	0.4	-.02	1.4	-.13	3.8	-.25
7	3	7.5	-2.95	3.9	-.71	5.7	-1.63	3.9	-.21
	6	9.1	-3.91	2.1	-.25	3.6	-.73	5.0	-.27
	18	5.6	-1.12	1.5	-.09	3.0	-.31	4.7	-.59
	21	3.2	-.69	2.7	-.38	2.3	-.36	11.4	-2.52
	24	8.3	-3.01	2.3	-.28	3.9	-.78	10.4	-1.36
10	24	6.4	-.62	0.3	-.00	0.7	-.02	0.8	-.00
11	24	39.8	-60.19	1.7	-.16	7.7	-1.94	12.9	-1.05
12	6	10.9	-4.28	1.5	-.14	8.9	-2.79	15.4	-1.18
	9	33.7	-26.39	4.2	-.53	7.8	-1.47	21.6	-.14
	21	6.7	-1.64	3.4	-.46	6.1	-1.38	12.4	-1.04
	24	18.3	-10.68	4.6	-.82	7.9	-2.29	10.6	-.76
13	3	41.3	-53.69	2.7	-.37	50.0	-84.80	4.1	-.23
	6	50.3	-105.80	1.6	-.17	6.8	-2.13	9.8	-.90
	18	31.7	-30.96	5.0	-.61	10.9	-2.53	4.4	-.31
	21	41.2	-64.05	5.7	-1.03	8.8	-2.47	1.4	-.03
	24	45.4	-86.96	2.8	-.41	12.8	-5.54	6.7	-.61
14	3	41.4	-79.30	1.4	-.14	8.1	-2.70	7.8	-.66
	6	41.7	-67.10	0.7	-.05	5.3	-1.23	13.1	-1.49
	21	13.4	-6.05	4.5	-.73	4.2	-.77	5.0	-.43
	24	16.3	-9.19	4.3	-.80	6.6	-1.92	8.0	-.97
16	24	4.9	-1.19	3.1	-.39	1.6	-.14	10.6	-1.18
18	24	37.9	-38.07	2.9	-.29	12.6	-3.47	13.5	-1.25
19	3	16.2	-8.41	2.3	-.23	4.4	-.78	11.4	-.92
	6	9.7	-3.43	1.6	-.13	2.5	-.33	10.0	-.68
25	21	11.4	-3.41	0.9	-.04	3.0	-.31	3.4	-.16
26	6	4.2	-.65	1.4	-.08	1.6	-.12	3.8	-.13
	21	14.3	-4.81	11.6	-2.17	10.8	-2.35	6.4	-.39
30	21	45.6	-39.00	10.0	-1.80	48.0	-42.00	14.1	-1.26
	24	50.4	-53.11	11.2	-2.42	47.0	-53.27	19.3	-1.65

APPENDIX II Cont'd

Day	Hour	Generalized Similarity		Rossby, h=1000 m		Rossby, h=500 m		Melgarejo & Deardorff (1975)	
		u_*	$Ho/\rho C_p$	u_*	$ho/\rho C_p$	u_*	$Ho/\rho C_p$	u_*	$Ho/\rho C_p$
31	3	45.9	-55.30	7.0	-1.32	17.9	-6.79	12.5	-.92
	6	44.8	-66.10	4.4	-.70	21.8	-10.86	13.4	-1.00
	21	12.0	-5.20	3.5	-.45	4.7	-.87	9.0	-.96
32	24	32.8	-58.34	4.3	-.69	7.5	-2.01	10.7	-.83
	3	4.1	-.88	1.6	-.15	3.2	-.55	7.2	-.40
	6	3.8	-.81	0.7	-.04	2.7	-.45	4.6	-.28
33	24	10.0	-4.88	0.8	-.04	2.4	-.33	4.8	-.33
	3	1.1	-.11	0.1	-.00	0.4	-.02	6.9	-.50
	18	5.9	-.99	1.5	-.08	3.0	-.26	8.1	-.91
34	21	14.1	-7.62	2.8	-.34	5.1	-1.07	4.6	-.34
	24	8.1	-2.94	3.5	-.56	6.4	-1.90	4.9	-.30
	3	8.0	-2.95	2.4	-.34	5.9	-1.75	7.3	-.57
35	6	2.2	-.32	2.1	-.27	2.8	-.48	11.7	-.74
	18	36.2	-27.52	13.7	-2.06	35.1	-22.35	15.2	-1.15
	21	38.5	-72.90	6.0	-1.19	10.5	-3.55	11.2	-1.00
39	6	60.3	-74.45	7.3	-1.51	54.1	-67.14	19.5	-2.15
	3	38.4	-35.01	1.8	-.14	20.6	-7.41	21.9	-.98
	24	0.7	-.00	0.6	-.00	.00	-.00	2.0	-.06
40	3	0.3	-.00	0.1	-.00	0.1	-.00	7.7	-.47
	21	6.1	-1.45	1.1	-.06	1.9	-.18	15.1	-1.73
	24	14.0	-7.06	2.3	-.25	2.6	-.34	14.7	-1.61
44	3	44.7	-64.83	4.2	-.67	12.8	-4.32	14.7	-1.88
	3	62.0	-19.19	61.2	-35.44	64.7	-25.16	26.6	-2.42
	6	69.1	-18.93	65.8	-28.41	69.0	-16.93	27.0	-2.73

UNSTABLE PERIOD

1	15	25.7	12.53	25.9	10.38	24.3	21.93	24.8	3.39
6	15	10.5	24.37	7.1	23.65	9.9	25.80	7.2	4.43
7	12	27.7	19.95	27.4	10.47	29.9	16.08	24.6	7.04
	15	20.3	15.65	21.7	14.12	20.0	16.67	18.8	4.58
12	12	26.6	12.03	25.7	9.38	28.5	17.09	27.1	7.97
13	12	24.6	17.77	15.4	8.24	24.8	18.87	35.5	11.75
	15	27.3	22.10	28.3	19.45	25.0	25.40	32.7	10.80
14	15	19.2	27.35	24.3	22.28	16.4	25.56	17.5	7.30
25	15	29.3	28.96	30.1	33.50	28.8	35.36	34.2	11.79
26	12	28.3	8.66	20.8	-.85	29.4	10.26	27.2	3.73
	15	27.6	7.36	28.5	7.03	28.4	7.77	24.9	3.55
33	9	12.7	16.64	8.6	-1.40	9.1	1.05	14.8	8.86
	12	17.5	76.71	17.5	76.71	14.5	74.45	14.0	15.86
	15	17.4	55.37	18.5	55.86	14.6	49.68	16.5	13.59
34	12	29.2	48.27	28.8	42.36	30.2	48.85	33.1	19.48
	15	28.6	53.80	30.1	52.93	29.5	50.41	31.5	17.91
35	12	37.2	27.64	36.9	22.02	36.9	32.59	43.2	16.93